Not for Publication

The Morphology of the Adult of the Larch Sawfly, *Pristiphora erichsonii* (Htg.) (Tenthredinidae, Hymenoptera)

by
H. R. Wong

Interim Report 1958 - 1
Forest Biology Laboratory
Winnipeg, Manitoba

Canada
Department of Agriculture
Science Service
Forest Biology Division

June 1958

A B S T R A C T

A detailed morphological study of the male and female of the larch sawfly, Pristiphora erichsonii (Htg.), is presented as a prelude to a study of the evolution of the genus, Pristiphora. The literature on sawfly morphology is reviewed. As a basis for future systematic and phylogenetic studies, special attention is given to descriptions of the genitalia of both the male and female. Some new terms are introduced for certain structures, previously undescribed in this group. Some structural variations in the larch sawfly are noted.

TABLE OF CONTENTS

1. INTRODUCTION

When one endeavours to extrapolate the evolution of a group of insects, considerable emphasis is placed on morphological conditions. This is understandable because morphology is essentially the study of the evolution of a structure, which is intimately correlated with function. Furthermore, inherent in groups of living insects are primitive and specialized characters, which will assist in reconstructing the probable paths of evolution. Morphological studies also help in orientating and naming the structures used in phylogenetic analysis.

At the present time, the external morphology has been described in detail for only four species of sawflies. These are Hoplocampa halcyon (Nort.) by Bird (1926), Diprion polytomum (Htg.) by Reeks (1937), Diprion pini (L.) by Arora (1953), and Cephalcia marginata Middlekauff by Rivard (1955). The general morphology of several sawflies has been described by other authors. Snodgrass (1933, 1935) has illustrated parts of Nematus ribesii (Scop.), Marlatt (1896) of Pachynematus erichsonii, and Smulyon (1923) of Tenthredo verticalis (Say). Parts of the anatomy of other sawflies have also been illustrated and described in the literature to indicate certain morphological features.

From the foregoing it can be seen that a study of the complete external morphology of any of the species in the genus Pristiphora is not available. Because of the writer's interest in the taxonomy and phylogeny of this genus, the need for a fairly complete morphological study of at least one representative species became readily apparent. The larch sawfly, P. erichsonii (Htg.) was chosen for this study because it is not only the most available species in this area, but it is one of the most economically important species in the genus that has a holarctic distribution.

No attempt is made to describe colour or size characteristics of the larval and adult stages in this paper. These have been already described by various authors, especially Packard (1890) and Hewitt (1912). The taxonomic history and biology of P. erichsonii (Htg.) has been reviewed by Coppel and Leius (1955).

The terminology and interpretations in this morphological study were made from the following sources: the basic morphology of sawflies, Snodgrass (1935); the comparative sawfly morphology, Ross (1937); the head of Hymenoptera, Bigelow (1954) and DuPorte (1946, 1957); the thorax of Hymenoptera, Richards (1956); the external genitalia of sawflies, Ross (1945); and the wing venation of sawflies, Ross (1936). The above information was supplemented by reference to Arora (1956) on the relationship of sawflies to other orders of insects; Michener (1944) on the comparative external morphology of bees; and Snodgrass (1956) on the anatomy of the honey bee.

2. THE FEMALE

2.1 The Head

The head of P. erichsonii (Htg.) is hypognathous. It is of the open head type with the occipital foramen continuous with the oral cavity. Ross (1937) referred to this as the simplest type of sawfly head from which all others are derived. It is roughly circular in outline, broader than long, and covered with short setae. The head is divided into definite areas by sutures or sulci. The sulci mark the position of internal ridges or inflections. From the cephalic aspect it is convex, with a conspicuous frontoparietal region. (Fig. 1, FP). According to DuPorte (1957), the frontoparietal region is a single sclerotized plate, which is partially divided ventrally by the frontogenal sulci (Fig. 1, FGS) defining a median lobe, the frons (Fig. 1, F), and the two lateral lobes are the genae (Fig. 1, GE).

The undivided dorsal area is the vertex (Fig. 1, VE). DuPorte's concept of the frontoparietal region ingores the cleavage lines because they are pale and without internal ridges. The frontogenal sulcus is very short, extending from the frontoclypeal sulcus (Fig. 1, FCS) to the antennal suture (Fig. 1, AS). The reduction of the area between the frontoclypeal sulcus and the antennal suture causes the short frontogenal sulcus and the small frons. The junction of the frontoclypeal sulcus and the frontogenal sulcus is marked by a deep invagination, the anterior tentorial pit (Fig. 1, ATP). Extending from the anterior tentorial pit to the anterior mandibular articulation (Fig. 6, AMA) is a smooth shiny groove called by Bigelow (1954) the clypeogenal bridge (Fig. 1, CGB). This bridge marks the division between the clypeus (Fig. 1, CL) and the gena. The clypeogenal bridge according to Bigelow (1954) "serves to cement and support the edges of the clypeus and genae when the latter descend below the original position of the mandibular articulations". Internally the clypeogenal bridge and frontogenal sulcus form inflections (Fig. 6, CGI, FGI) that are intimately associated with the anterior tentorial arm (Fig. 6, AT). Bigelow (1954) believes the frontoclypeal inflection originated as a reinforced region between the tentorial pits because of the stresses applied to the tentorial arms by muscles attached to them. As suggested by DuPorte, the anterior tentorial arms with the frontoclypeal inflection and the clypeogenal inflection apparently form a supporting structure, which counteracts the pull of the mandibles. The relatively large oval antennal sockets (Fig. 1, ANTS) are situated in the centre of the frontoparietal region. On the ventromesal margin of the antennal socket is an elongate antennifer (Fig. 1, AN), which articulates with the antenna. Immediately above the antennal socket is a smooth triangular depressed area, the tentorial macula (Fig. 1, TM), marking the external position of the dorsal tentorial arm. A protuberance between

the antennal sockets defines the median crest, on which is a small elongate depression called the median fovea. The compound eye (Fig. 1, CE), occupying most of the lateral margin, protrudes slightly from the side of the head. The ocular suture (Fig. 1, OS), which in more generalized insects surrounds the compound eye, is distinct only on the caudal margin.

A slightly raised rectangular area on the dorsal part of the head is referred to as the postocellar area (Fig. 1, POA) by some taxonomists, and the vertex by Arora (1953). This is marked laterally by the lateral sulcus (Fig. 1, LS) or temporal suture and ventrally by a shallow groove, the transverse suture (Fig. 1, TS), which joins the ventral ends of the lateral sulci. The lateral sulcus extends from the lateral ocellus (Fig. 1, LO) to near the caudal margin of the head. The lateral inflection continues internally as part of the tentorial thickening (Fig. 6, TT) to the tentorial bridge (Fig. 6, TB). The rudimentary coronal suture (Fig. 1, CS) bisects the transverse suture, and extends dorsally into the postocellar area. The frontal suture (Fig. 1, FS) extends from the ventral end of the coronal suture for a very short distance on either side of the median ocellus (Fig. 1, MO), but not beyond it. The three ocelli form a triangle with the median ocellus in a slight depression referred to as the ocellar basin.

Below the frons is the narrow clypeus (Fig. 1, CL), which is enclosed between the genae, and extends to the anterior articulation of the mandibles (Fig. 6, AMA). It is separated from the frons (Fig. 1, F) by the frontoclypeal sulcus (Fig. 1, FCS); from the gena (Fig. 1, GE) by the clypeogenal bridge (Fig. 1, CGB); and from the labrum (Fig. 1, LA) by the clypeolabral suture (Fig. 1, CLS). The clypeus is about three times broader than long with the distal margin very slightly emarginate to straight, and covered with setae, which are longer than those on the frontoparietal region. The

labrum which overhangs the oral cavity, is not as broad as the clypeus. It is a setiferous rectangular structure about twice as broad as long, with the distal margin almost straight. The tormae (Fig. 8, TOR) are concealed behind the clypeus on the dorsolateral angle of the labrum as a pair of narrow sclerites, which are directed caudally and associated with the pharyngeal sclerite (Fig. 8, PHS). This sclerite is deeply bifid at the dorsal end, and punctate laterally. The inner surface of the labrum or epipharynx is rugose and sparsely setiferous.

The head is concave caudally with an elongate occipital foramen (Fig. 2, OCF). The tentorial bridge (Fig. 2, TB) extends across the occipital foramen. As indicated by Ross (1937) for all adult sawflies, the occipital and occipitopostgenal sutures are absent, making it difficult to differentiate the genae and postgenae. The crassa is also absent. The occipital foramen is surrounded dorsally and laterally by the postoccipital sulcus (Fig. 2, POS), to which is attached the neck membrane. The sulcus cuts off a narrow horseshoe-shaped postocciput (Fig. 2, PO), and defines the occiput (Fig. 2, OC) dorsally and the postgena (Fig. 2, PG) laterally. Two diverging sulci called tentorial thickenings (Fig. 2, TT) outline the lateral boundaries of the occiput. On the dorsomesal angle of the postocciput is a small process directed ventrally. The odontoidea (Fig. 2, OD) or occipital condyle projecting from the post-occiput is borne by the maxillaria (Fig. 2, MX). It articulates with the cervical sclerite (Fig. 15, CSC). On the ventral margin of the maxillaria is the paracoila (Fig. 2, PAC), with which the maxilla articulates. The posterior tentorial pit (Fig. 2, PTP) is somewhat triangular and situated at the lower end of the postoccipital sulcus. The hypostoma (Fig. 2, HST) is weakly indicated on the ventral edge of the postgena by an oblique hypostomal suture (Fig. 2, HS), which extends toward the maxillaria.

2.1.1 The Tentorium

The tentorium is a well-developed sclerotized structure. It consists of two lateral plates, which are united across the occipital foramen by the tentorial bridge (Fig. 2, TB), and paired tentorial arms. The posterior tentorial arms, which arise from the posterior tentorial pits (Fig. 2, PTP) at the lower ends of the postoccipital sulcus, extend mesad to form the tentorial bridge (Fig. 6, TB) in front of the odontoidea. The anterior tentorial arms (Fig. 6, AT) extend caudally and dorsally from the anterior tentorial pits (Fig. 1, ATP) at each end of the frontoclypeal sulcus to the cephalic part of the tentorial bridge and fusing with the maxillaria. The slender dorsal tentorial arms (Fig. 6, DT) are apparently secondary outgrowths of the anterior tentorial arms. They extend to the inner wall of the cranium above the antennal sockets. The position of the dorsal tentorial arms is marked externally by the tentorial maculae.

2.1.2 The Appendages of the Head

The appendages of the head include a pair of antennae, a pair of mandibles, a pair of maxillae, and the labium. The maxillae and the labium are united along the postmentum (Fig. 2, PM) of the latter and the mesal margin of the cardo and stipes of the former (Fig. 2, CD, ST) to form a composite structure.

The antennae are covered with numerous fine setae and stout spines. Each antenna consists of a quadrate scape (Fig. 9, SC) which has a light coloured suture in a slight constriction on the basal part cutting off the bulbus (Fig. 9, BL); the pedicel (Fig. 9, PD), containing the Johnston's organ, is wider than long and expanded apically; the flagellum (Fig. 9, FL) contains seven elongate segments, with the basal segment slightly curved.

The mandibles (Fig. 5) are dicondylic, flattened sclerotized structures, that taper apically to a point. They possess an abundance of setae laterally, and two dentes, a long slender lateral tooth and a very short stout mesal tooth. The left and right mandibles are dissimilar. The lateral tooth is longer on the left mandible, and the mesal tooth is longer on the right mandible.

The setiferous maxilla consists of a triangular cardo (Fig. 2, CD) and elongate stipes (Fig. 2, ST). The cardo is produced proximally into a process for articulation with the paracoila (Fig. 2, PAC) of the maxillaria and directed mesally towards the postmental sclerite (Fig. 2, PMS). Distad of the cardo is the stipes (Fig. 2, ST), which bears laterally the 6-segmented setiferous maxillary palpus (Fig. 2, MXP), the basal segment being the palpifer (Fig. 3, PFR). The proximal three segments of the palpus are more highly sclerotized than the distal three; the latter are lighter in colour and are more sparsely covered with setae. The stipes bears terminally the galea (Fig. 3, GL), and mesally the lacinia (Fig. 3, LC). The galea is an ovate lobe with long scattered setae on the lateral surface, and short setae on the mesal surface. The lacinia is a long narrowly tapered structure that is pressed against the galea. It possesses numerous short setae interspersed with long setae.

The labium consists of a membranous rectangular proximal postmentum (Fig. 2, PM), and a sclerotized distal prementum (Fig. 2, PRM). The postmentum bears a heart-shaped setiferous sclerite between the mesally directed angles of the cardines. This sclerite corresponds with the submentum of Ross (1937) and Reeks (1937). Arora (1953) calls it the postmental sclerite (Fig. 2, PMS) because in certain sawflies such as Megalodontes klugii (Leach)

there are three such sclerites. The prementum is roughly M-shaped and bisected by a vertical sulcus with setae on the distal half of the adoral surface. The distal end of the prementum bears three terminal lobes. The narrow, elongate median lobe represents the fused glossae or the alaglossa (Fig. 2, AGL), and the deltoid lobe on each side is the paraglossa (Fig. 2, PGL). The adoral surface of the alaglossa (Fig. 2, AGL) is characterized by sclerites at the proximal end, and setae on the distal end. The paraglossa has also very narrow sclerites situated at the proximal end and the lateral margin of the adoral surface (Fig. 2), with setae on the distal end. The prementum carries the 4-segmented setiferous labial palpus (Fig. 4, LP) laterally. The first segment, or the palpiger (Fig. 4, PGR), and the second segment are moderately sclerotized and slightly tapered. The remaining two segments are lightly sclerotized and more rounded. The oral surface of the paraglossa and alaglossa have rows of very short setae on the distal half, and a few scattered longer setae on the proximal half.

The hypopharynx (Fig. 4, HP) is represented by a raised lobe on the oral surface of the prementum, situated at the proximal end of the alaglossa. The distal end of the hypopharynx bears numerous small setae.

2.2 The Thorax

The thorax of the larch sawfly consists of three segments, the pro-, meso and metathorax. The wing-bearing segments are referred to as the pterothorax.

2.2.1 The Prothorax

Joining the head to the prothorax is a membrane called the cervix or cervical membrane. The tergum or notum of the prothorax, referred to as the pronotum (Figs. 11, 15, PRN), is covered with setae and separated from the pleurosternal parts of the prothorax. It is a collar-like plate, very

closely associated with the mesothorax. The top of the collar is narrowed, with the sides expanded into a broad triangular plate above the cervical sclerite (Fig. 15 CSC). The caudoventral angle of the pronotum extends to the cephaloventral corner of the epicnemium (Fig. 15, EPC_2) and the presternum (Fig. 15, PES_2). The caudodorsal angle of the pronotum is recessed to form a pronotal lobe (Fig. 15 PN) for the reception of the cephalic margin of the tegula (Fig. 11, TG). The pronotal lobe extends internally near the dorsal margin as a pronotal inflection to form an internal ridge that narrows gradually towards the mediocephalic margin of the pronotum. The cephalic margin of the pronotum is grooved by a transverse furrow, which is marked internally by a transverse ridge.

The roughly triangular lateroventral sclerite, which is ventrad of the pronotum, has been known as the cervical sclerite, but more recently called the propleuron (Richards, 1956; Snodgrass, 1956). It is convexly curved and covered with setae. Extending dorsad from the lateral coxal articulation of the prothoracic leg is the pleural sulcus (Fig. 15, PLS_1), which cuts off a narrow caudal epimeron (Fig. 15, EPM_1) and a large cephalic episternum (Fig. 15, EPS_1). When the propleuron is fully exposed, the apical cephalic margin appears to flare into a pair of pointed processes (Fig. 7, e, d). The anterior process (Fig. 7, e) of the episternum articulates with the odontoidea on the back of the head. The posterior process (Fig. 7, d) of the episternum is for the attachment of muscles. On the dorsocaudal margin of the episternum, next to the pleural sulcus, is a broad apodemal ridge (Fig. 7, c) that extends entad and ventrad. The basisternum (Fig. 10, BS) is a roughly T-shaped sternal plate, which is divided longitudinally by a central invagination similar to the discrimen of the mesosternum. The basisternum is slightly concave, extending caudally into a narrow invaginated

bifid furcasternum (Fig. 10, FRS_1) of the prothorax. The precipitous lateral edges of the furcasternum has a mesosternal articulation with the coxa of the prothoracic leg. Internally a slight ridge at the cephalic margin of the basisternum is visible. It is bisected by a median longitudinal invagination called the vertical plate of the proseternal apophysis (Fig. 7, VPA_1) which increases in height caudally. Near the centre of the basisternum, and supported by the vertical plate is a horizontal plate (Fig. 7, HPA_1) of the prosternal apophysis, which widens toward the arms of the endosternum (Fig. 7 EOS_1). In some specimens of the larch sawfly the basisternum is only partly divided (Fig. 10a) longitudinally. The central invagination diverges near the caudal portion of the basisternum, enclosing a narrow central portion of the basisternum (Fig. 10a, CBS). Internally this central portion produces two vertical lamellae of the prosternal apophyses, which merge caudally at the base of the endosternum. Arising from the furcasternum is a large elaborate endosternum (Fig. 7, EDS_1) also called the furca. The endosternum is supported by a median stalk that diverges into a U-shaped bridge on which is a triangular-shaped apophysis. From this apophysis can be seen a long muscle apodeme (Fig. 7, MUP). Extending caudally and dorsally into the body cavity from the epimeron and ventral end of the pleural sulcus is a large internal apodemal arm, the pleural arm (Fig. 7, PLA_1), which is intimately associated with the endosternum. Lying in the membrane between the episternum and the end of the horizontal part of the basisternum is a small narrow setiferous sclerite, the trochantin (Fig. 10, TRO_1). Caudad of furcasternum is the narrow triangular spinasternum (Fig. 10, SS) which abuts the cephalic margin of the presternum (Fig. 10, PES_2) of the mesothorax. Internally the spinasternum produces a spatulate spina (Fig. 18, SPN).

2.2.2 The Mesothorax

The setiferous mesothorax is the largest segment of the thorax. The dorsum is convex and consists of the notum, or alinotum, and the postnotum. The alinotum is composed of the prescutum or praescutum (Fig. 11, PRS) of Ross (1937), the scutum (Fig. 11, $SCUT_2$) and the scutellum (Fig. 11, SCL_2). The prescutum is roughly triangular with sloping sides. The cephalic margin of the prescutum is deflected to form a bifid first phragma or prephragma (Figs. 11, 16, PH_1). The lateral margin is defined by a pair of converging sulci or notaulices (Fig. 11, NO), that meet at a mid line. Internally the notaulices form converging ridges (Fig. 16, CR) that are more prominent at the cephalic margin and diminish in depth toward the caudal margin. A median sulcus (Fig. 11, MS) extends to about the middle of the prescutum. Internally it forms the median ridge (Fig. 16, MR) that attains its greatest prominence at the cephalic end. Part of the cephalolateral margin of the prescutum and the scutum is extended outward and slightly inflexed to form a narrow lateral process, the anterolateral mesoscutal process (Fig. 11, ASP). Internally this process is confluent with a transverse anterolateral mesoscutal inflection (Fig. 16, ASI), cephalad of the anterior notal wing process. This inflection rests against the pronotal inflection along the caudodorsal margin of the pronotum. Along the sides and just caudad of the prescutum to the scutellum (Fig. 11, SCL_2) is the scutum (Fig. 11, $SCUT_2$). The lateral margin of the scutum is produced outward to form the anterior notal wing process (Fig. 21, ANP_2), and the posterior notal wing process (Fig. 21, PNP_2). The anterior notal wing process is slightly emarginated to produce a lobe-like cephalic part, and a caudally projecting part. Behind the caudal projection of the anterior notal wing process is a slight curved fissure (Figs. 11, 21, I_2) on the edge of the scutum. This fissure has been referred to by Snodgrass (1935, Fig. 101,

I) as the posterior intrascutal groove. The posterior notal wing process is not differentiated. Internally there is present a lateroposterior mesoscutal inflection (Fig. 16, LSI) behind the scutal fissure. The parapsis (Fig. 11, PAR) or the parascutellar area is a decidedly declivous caudolateral area of the scutum. This area is indicated cephaladly by the diagonal parapsidal furrow (Fig. 11, PF). The scutellum is separated from the scutum by an inverted V-shaped external notal sulcus (Fig. 11, ENS) or the scutoscutellar sulcus. This groove marks a prominent internal notal ridge (Fig. 16, INR_2), which is more deeply inflected at the caudal margin and tapers towards the meson. In front of the internal notal ridge are two narrow lightly sclerotized areas. The caudal area of the scutellum is separated into a triangular posttergite (Fig. 11, PTG) by the conspicuous posterior marginal fold of the scutellum (Fig. 16, RD_2). The lateral margin of the posttergite is continuous with the axillary cord of the wing.

Behind and partially hidden by the alinotum and metanotum is the postnotum (Fig. 11, PTN_2). It is a broad sclerotized roughly W-shaped collar that is united laterally to the epimeron of the mesothorax, and connected to the alinotum by a membrane. Externally a narrow membrane between the posttergite and the scutum of the metathorax appears to divide the postnotum into two parts. The posterior margin of the postnotum is produced caudally and ventrally beneath the metatergum and part of the first abdominal tergum to form a large bifid second phragma (Fig. 11, PH_2) or postphragma. Along the cephalic border of the second phragma is a transverse posterior lip (Fig. 11, L), which is slightly vertical in position. This posterior lip according to Snodgrass (1935) is the phragmatal inflection behind the antecostal suture.

On the upper part of the pleuron of the mesothorax is the oblique

pleural sulcus (Fig. 15, PLS_2) running dorsad and cephalad from the lateral coxal articulation of the second coxa to the anterior pleural wing process (Fig. 15, WP_2). The pleural sulcus divides the pleuron into the dorsal epimeron and the ventral episternum. The epimeron is divided by an epimeral sulcus (Fig. 15, ES_2) into a narrow oblong cephalic anepimeron (Fig. 15, AEM_2) and a roughly L-shaped caudal katepimeron (Fig. 15, KEM_2). The dorsal area of the anepimeron has a transverse sulcus which is deeply impressed by a subalar pit (Fig. 15, SAP). The katepimeron has the dorsal margin slightly reflected. The episternum is also differentiated into two parts. A triangular dorsal cephalic piece between the pleural wing process and the mesothoracic spiracle (Fig. 15, SP_1) has been called by Michener (1944) the postspiracular sclerite. This is believed to be a fragmentum of the mesepisternum. Arora (1953) calls it the anepisternum (Fig. 15, AES_2) and says "this piece can safely be compared to the anepisternum of the Neuroptera, in which the division of the episternum into an anepisternum and katepisternum is a common feature". Richards (1956) believes that it is probably the anepisternum. The large rectangular area caudad of the anepisternum is the katepisternum (Fig. 15, KES_2). The dorsocephalic corner of the katepisternum in front of the subalar pit is marked by a pleural cleft (Fig. 15, PC). The cephaloventral corner of the katepisternum is marked by the anterior oblique sulcus (Fig. 15, AOS_2), which extends ventrad from the anepisternum to meet the median longitudinal discrimen (Fig. 10, DCM_2). This sulcus cuts off an elongate triangular presternum (Figs. 10, 15, PES_2) or prepectus. Just ventrad of the anepisternum and cephalad of the presternum is a very narrow sclerite, the epicnemium (Fig. 15, EPC_2), which is defined by the epicnemial sulcus (Figs. 15, 20, ESU_2). Internally the pleural sulcus forms a strong pleural ridge (Fig. 18, PLR_2). The epimeral ridge (Fig. 18, ER) abutting the

pleural ridge is wider at the ventral than at the dorsal end, and is continuous at right angles with the pleural arm (Fig. 18, PLA_2) of the mesothorax. The pleural arm arises laterally as an internal apophysis at the junction of the postnotum (Figs. 15, 18, PTN_2) with the katepimeron (Figs. 15, 18, KEM_2). It projects entad and caudad above the endosternum (Fig. 18, EDS_2). Extending across the dorsal area of the epimeron, from the epimeral ridge to the dorsal end of the pleural ridge, is a transverse dorsal mesepimeral inflection (Fig. 18, DMI), which surrounds the external elongate subalar pit. A very short inflection (Fig. 18, R) behind the vertical epimeral ridge appears to be connected to the transverse dorsal mesepimeral inflection across the epimeral ridge. At the cephalic end of the transverse dorsal mesepimeral inflection and the pleural ridge is an anterior pleural apodeme (Fig. 18, AKA). Behind the anepisternum or the postspiracular sclerite is a large ovoid muscle-bearing disk (Fig. 18, G), which is notched along the mediocaudal margin and appears to be connected to the anepisternum. According to Michener (1944) the disk is united to the lower margin of the true basalare by a tendon-like apodeme. The anterior oblique sulcus is indicated internally by the anterior oblique ridge (Fig. 18, AOR_2) on the cephalic sternopleural aspect of the mesothorax. The two anterior oblique ridges meet ventrally and join the vertical plate of the mesosternal apophysis (Fig. 18, VPA_2), forming the horizontal plate of the mesosternal apophysis (Figs. 18, 19, HPA_2). In front of the anterior oblique ridge is the epicnemial ridge (Fig. 18, EPR_2), which has a sharply pointed anterior presternal apodeme (Fig. 18, APA) on its ventral end. This apodeme is directed cephalad beyond the epicnemium to the pronotum.

The episternum extends ventrally to the discrimen (Fig. 10, DCM_2) making it difficult to distinguish the basisternum (Fig. 10, BS_2) from the

episternum of the mesothorax. The discrimen is a central longitudinal line on the basisternum. Along the discrimen is a long narrow discrimenal pit (Fig. 10, DP_2), which occupies the median area of the basisternum. It has been suggested that the episterna has actually extended to the discrimen, and the true sternum has infolded to form the endosternum (Fig. 18, EDS_2). Snodgrass (1956) does not concur with this interpretation, and believes that "there is no reason why the cuticular sclerotization may not become confluent where continuity gives some mechanical advantage". The discrimen is marked internally by the inflected vertical plate of the mesosternal apophysis (Figs. 18, 19, VPA_2). The vertical plate is decidedly higher at the caudal end than the cephalic end, and appears to be reinforced by diagonal sutures. The endosternum arises at the caudal area of the vertical plate as two divergent arms on a common stalk from the furcasternum of the mesothorax. At the distal end of each arm are five finger-like divergent processes. The middle process is the longest and extends toward the pleuron. Along the top of the vertical plate of the mesosternal apophysis is the horizontal plate (Fig. 19, HPA_2) of the mesosternal apophysis. This plate has a wide constriction in the central area. Behind the basisternum is the small furcasternum (Figs. 10, 18, FRS_2), which projects caudally as a pair of processes. Arora (1956) has indicated that the forecoxa of sawflies has a pleural articulation and usually a sternal articulation, while the meso- and metacoxa have a pleural, a sternal and a trochantinal articulation. The trochantin (Fig. 18, TRO) in the larch sawfly is rudimentary and is fused with the sternum, making it difficult to observe the trochantinal articulation. It can best be seen in lateral view, situated ventrad and slightly cephalad of the furcasternum (Fig. 18, FRS_2). A divergent process of the furcasternum and the rudimentary trochantin appear as one unit,

with the extreme caudal end bending slightly laterad to articulate with the mesoproximal margin of the coxa. The mesosternum does not bear an internal spina. According to Arora (1953 and 1956) the mesosternum of sawflies he studied bears a membranous spinasternum lying behind the legs and the divergent processes of the furcasternum. He stated that it can best be seen when the legs are pulled up and apart.

2.2.3 The Metathorax

The more sparsely setiferous metathorax is considerably smaller than the mesothorax and does not possess a prescutum. The scutum (Fig. 11, $SCUT_3$) is very narrow medially, and enlarged laterally to produce the anterior and posterior notal wing processes (Fig. 25, ANP_3, PNP_3). The cephalic margin of the scutum is deflected (Fig. 17), with the deflection being more pronounced towards the sides. The cephalolateral corner of the scutum has a pointed lateral and mesal process. The lateral process is the anterior notal wing process (Fig. 25, ANP_3). The mesal process, which extends ventrad is connected with the inter-segmental membrane. Behind the lateral process is a curved fissure on the edge of the scutum (Figs. 11, 25, I_3). This scutal fissure, also called the posterior intrascutal groove, is larger and more rigid than that of the mesothorax. The greater part of the lateral area of the metascutum, with the exception of a narrow cephalic area, is declivous. This would correspond to the parapsis and the parapsidal furrow of the mesonotum. On the narrow raised cephalic portion of the scutum is a pair of slightly elevated opaque areas, the cenchri (Figs. 11, 25, CN). These are ovate and narrowed toward the meson. Because of the deflected cephalic margin of the scutum, the cephalic edge of the cenchri appear to extend beyond the cephalic margin of the scutum in dorsal

view. The scutum is separated from the scutellum (Fig. 11, SCL_3) by a deep external notal sulcus or scutoscutellor sulcus. This sulcus is relatively straight with the extreme ends bent sharply toward the cauda. Internally this is indicated by the internal notal ridge (Fig. 17, INR_3) or scutoscutellor ridge. On top of this ridge on either side beyond the middle is a ledge, which gradually widens toward the sides. The scutellum is narrow and rectangular in shape. Latterally, it is continuous with the axillary cord of the hind wing. The caudal margin of the scutellum is deflected to form a prominent posterior marginal fold (Fig. 17, RD_3), which meets latterally with the internal notal ridge. The posterior marginal fold of the alinotum supports a narrow ledge, which widens laterally and joins the widened ends of the ledge of the internal notal ridge. The postnotum (Fig. 11, PTN_3) is caudad of the scutellum. It is a narrow collar with an angulated cephalic margin. Internally the cadual margin of the postnotum is deflected to form a very narrow rudimentary third phragma (Fig. 17, PH_3), which is not bifid. The caudolateral margin of the postnotum has a small rectangular tergal apodeme (Fig. 17, TAP) internally, which extends ventrad and slightly cephalad. This apodeme was referred to as the third phragma by Reeks (1937).

The pleural sulcus (Fig. 15, PLS_3), indicated internally as the pleural ridge (Fig. 18, PLR_3), runs dorsad and cephalad from the lateral articulation with the third coxa to the posterior pleural wing process (Fig. 15, WP_3). It divides the metapleuron into the dorsal epimeron and a ventral episternum. The epimeron (Fig. 15, EPM_3) is not completely divided as in the mesopleuron. A rudimentary epimeral sulcus (Fig. 15, ES_3), which normally divides the epimeron into the anepimeron and the katepimeron is present on the ventral margin as a stub just above the anterior oblique sulcus (Fig. 15, AOS_3). The dorsal margin of the epimeron is greatly sinuate.

That portion cephalad of the katepisternum (Fig. 15, KES_3) is deeply emarginate, while the area behind this emargination slopes toward the caudal margin. The episternum is divided into a large rectangular katepisternum (Fig. 20, KES_3), and a very narrow elongate anepisternum (Fig. 20, AES_3) behind the metathoracic spiracle (Fig. 20, SP_2). A much smaller and narrow sclerite is present in the membrane between the metathoracic spiracle and the anepisternum. This sclerite is possibly the detached epicnemium (Fig. 20, EPC_3) of the metapleuron. The episternum extends ventrally to the discrimen (Fig. 10, DCM_3), the central longitudinal line of the metaventrum. This condition as in the mesothorax causes the episternum to be fused with the basisternum. The anterior oblique sulcus (Fig. 15, AOS_3) at the cephalic margin of the katepisternum, extends ventrally from the pleural sulcus to the discrimen. This marks off a narrow presternum (Figs. 10, 15, PES_3), which decreases in width ventrally. Internally the anterior oblique sulcus is indicated by the anterior oblique ridge (Fig. 19, AOR_3), which is more pronounced laterally than ventrally. The junction of the pleural ridge, rudimentary epimeral ridge, and the anterior oblique ridge marks the location of a short internal apophysis, the pleural arm (Figs. 18, 19, PLA_3). The apical end of the pleural arm is flared and twisted. It projects entad and ventrad above the endosternum (Fig. 18, EDS_3) of the metathorax. The discrimen is short and slightly elevated caudally on the basisternum (Fig. 10, DCM_3). The discrimenal pit (Fig. 10, DP_3) at the cephalic end is triangular-shaped. On either side of the elevated portion of the discrimen is a shallow declivous area. The discrimen is marked internally by the short vertical plate of the metasternal apophysis (Fig. 19, VPA_3), with the endosternum (Figs. 18, 19, EDS_3) arising at the cephalic end of the basisternum. The arms of the endosternum arise from a

common stalk, and are wing-like with four short processes. As in the mesosternum, the metasternum has a rudimentary trochantin fused with the sternum, providing pleural, sternal, and trochantinal articulations to the metacoxa.

2.2.4 The Appendages of the Thorax

Each thoracic leg is setiferous and consists of the following parts (Fig. 12): coxa (CX); trochanter (TR), (which appears to be 2-segmented); femur (FM); tibia (TI); tarsus (TAR); and pretarsus (PRT). The legs are similar, but differ in size and shape of some of the parts. Sense organs or proprioreceptors are evident on the legs, but they are not described in this paper. The proximal segment of the leg is the coxa. It has two points of articulation in the prothoracic leg: a pleural articulation with the ventral end of the pleural sulcus, and a sternal articulation with the caudal process of the furcasternum. The coxa of the prothoracic leg is subquadrate. The laterodistal surface of the coxa has a conical membranous area. Around the proximal end is a thickened marginal ridge, the basicoxite (Fig. 12, BSC). The coxa has cephalic and caudal points of articulation with the trochanter. These are indicated by short vertical sulci (Fig. 12, SUL) at the distal end of the coxa. The trochanter is small, slightly broadened distally, with the mesal surface curved and longer than the lateral surface. The distal margin of the trochanter has a faint circular suture. The femur has the proximal area marked off by a suture, and is attached to the trochanter. The close association of the conical proximal piece of the femur with the trochanter gives the impression that the latter is 2-segmented. The femur is an elongate segment, with a conical membranous area on the mesodistal surface. The tibia is slightly shorter than the femur. It has

a broad distal end and a groove on the cephalic surface. Two slender sharply pointed spurs (Fig. 12, TIS) are located on the broad distal end of the tibia. The cephalic spur is slightly curved and longer than the caudal spur. The tarsus is slender and elongate. It is longer than the tibia in the prothoracic leg, and consists of five tarsomeres, which are widened distally. The first subsegment or basitarsus is the longest. The fifth subsegment or distitarsus is shorter than the basitarsus, but longer than the subsegments two, three, and four, which constitute the mediotarsus. The subsegments of the mediotarsus are progressively shorter from two to four. The tarsal pulvillus (Fig. 12, TP) is an oval pad situated on the mesodistal surface of the basitarsus and mediotarsus. The pretarsus (Fig. 12, PRT) is the terminal segment of the leg. It consists of a pair of setiferous claws (Fig. 13, CW) or ungues, which articulate dorsally to the unguifer (Fig. 13, UF), a small bilobed plate at the distal end of the distitarsus. Each claw is slightly curved, broadened at the base, with a subtooth at the ventrodistal end. The orbicula (Fig. 13, ORB) extends from the apical emargination of the unguifer as a dorsal elongate sclerite, which is setiferous and bifid at the apical end. The lateral margins of the orbicula are heavily pigmented, with two pairs of long setae arising from the lateral area. Ventrally the unguitractor plate (Fig. 14, UTP) is a rectangular sclerite with a slight notch at the proximal margin, situated distad of the distitarsus. It is sculptured and setiferous. The proximal end of the unguitractor plate is attached to a tendon-like apodeme which extends through the tarsus. The quadrate planta (Fig. 14, PL) is distad of the unguitractor plate. It is slightly emarginate at the proximal margin and possesses several setae. On either side of the unguitractor plate is a small narrow sclerite known as the auxilia (Fig. 14, AU) or basipulvillus beneath the

base of the claw. The distal membranous adhesive lobe is the arolium (Fig. 14, AR). It is rounded in outline and supported dorsally by the orbicula, and ventrally by the planta. The arolium is strengthened near its base by a U-shaped sclerotic band, the camera (Fig. 14, CA). In dorsal view the arolium has a cavity between the upturned lateral walls. Above the camera and next to the distal end of the orbicula is a vertical sclerotized plate (Fig. 13, SPL), which is triangular in shape.

The meso- and metathoracic legs differ from the prothoracic legs chiefly in size, shape, and number or articulations. Pleural, sternal, and trochantinal articulations occur on the meso- and metacoxae, whereas only two articulations occur on each procoxa. The mesocoxa is subconical and longer than the procoxa. The metacoxa resembles the mesocoxa in shape, but is larger in size. The mesofemur is slightly longer than the profemur, and the metafemur is longer than the mesofemur. The mesotibia is about the same length as the mesofemur, but the metatibia, however, is longer than the metafemur. The tibial spurs on the meso- and metatibia are straight. The cephalic tibial spur on the mesotibia is only slightly longer than the caudal spur. The cephalic tibial spur on the metatibia on the other hand is shorter than the caudal spur. The tarsus and tibia of the mesothoracic leg is subequal, while the tibia is longer than the tarsus in the metathoracic leg.

The two pairs of membranous wings are hyaline and spinulate. When in flight the hamuli (Fig. 27, HU) along the cephalic margin of the hind wings are hooked onto a coupling fold (Fig. 22, CF) along the caudal margin of the front wings.

The front wing is elongate widening distally, and strengthened by setiferous veins and crossveins. The cephalic and caudal margins are relatively straight, with the distal margin tending to curve. Above and cephalad of the base of the wing is a quadrate, setiferous, sclerotized plate, the tegula (Fig. 21, TG). Caudad of the tegula there is an irregular sclerotization of the wing base called the humeral complex (Figs. 21, 22, HC) by Snodgrass (1956). This apparently is formed by the enlargement and union of the bases of C, R + Sc and M + Cu_1. It has ventral processes on the underside. Proprioceptive organs (Fig. 21, PCO) are present on the humeral complex. Four axillary sclerites and a median plate are situated in the basal membranous area of the front wing. The first axillary (Fig. 21, 1 AX) is a large sclerite occupying an oblique position. It has four processes. The cephaloproximal process forms a long neck, which rests on the cephalic portion of the anterior notal wing process (Fig. 21, ANP_2). The apex of the cephaloproximal process abuts the humeral complex. The mediopro**x**imal process is a vertical projection and rests on the caudal portion of the anterior notal wing process. The caudoproximal process is on the lateral margin of the scutum (Fig. 21, $SCUT_2$). The distal process is directed ventrad towards the central area of the second axillary (Fig. 21, 2 AX). The second axillary is a triangular sclerite, which occupies a vertical position in the wing base. It has a notch on the distal margin and a long caudal ridge on the dorsal surface of the proximal area, which is associated with the cephalic process of the third axillary (Fig. 21, 3 AX). On the ventral side of the second axillary is a shorter cephalic ridge near the proximal edge, associated with the pleural wing process. The cephalic end of the second axillary is flexibly connected to the common base of veins R + Sc and M + Cu_1. The third axillary is an elongate forked sclerite.

It has three processes, and occupies an oblique position in the wing base. The cephalic process is the largest with a deep notch along the lateral margin, and articulates with the second axillary. The caudal process articulates with the bases of the anal veins. The proximal process articulates with the fourth axillary (Fig. 21, 4 AX), which maybe a detached piece from the posterior notal wing process. In addition to being narrow and elongate, the fourth axillary is irregular in shape, articulating with the proximal process of the third axillary, and the posterior notal wing process (Fig. 21, PNP_2). The median plate (Fig. 21, MP) is narrow and elongate. It lies in the median area of the wing base, in front of the second axillary, and between the humeral complex and the first anal vein (Fig. 21, 1 A). The distal end of the median plate has a ventral process. Between the third axillary and the axillary cord (Fig. 21, AXC) is a small triangular-shaped sclerotized plate (Fig. 21, f). The axillary cord is a thickened corrugated ligament at the caudal edge of the wing, and is continuous with the lateral prolongation of the scutellum.

Beneath the base of the front wing are small sclerites called epipleurites. They are situated on either side of the pleural wing process. The sclerite cephalad of the pleural wing process, and above the anepisternum or postspiracular sclerite, is the basalare (Fig. 20, BA_2). It is a hammer-like structure with an elongate concavity in the central area and a notch on the caudal margin. Caudad of the pleural wing process is situated a narrow elongate sclerite, with a ventral process. This is the subalare (Fig. 20, SU_2), which is intimately associated with the proximal margin of the second axillary sclerite.

The costa (Fig. 22, C), running along the cephalic margin of the front wing, is strongly swollen at the apex. The stigma (Fig. 22, STG) or pterostigma is a dark elongate area situated near the centre of the costal margin. A very small rectangular weakened area, called bulla is present between the thickened end of the costa and the stigma. The costa is united to the common basal vein of R + Sc and M + Cu_1 at the base of the wing to form the humeral complex. The costa apparently has two areas of union, one proximad of the division of the R + Sc from M + Cu_1, and one at the base of the wing. The base of the costa appears to have fragmented into a very small distal sclerite (Fig. 21, a) and a larger proximal sclerite (Fig. 21, b) on the cephalic border of the humeral complex. The proximal costal sclerite (b) has a ventral process at the proximal end, and together with another ventral process of the humeral complex articulate with the sides of the basalare. Caudad of the costa (Fig. 22) is the common basal vein of R + Sc and M + Cu_1. The cephalic vein R + Sc is thicker than the caudal vein M + Cu_1. The subcosta (Fig. 22, Sc) extends cephalad after separating from the common vein R + Sc before the thickened end of the costa. The radius extends distad of the subcosta to join the media (Fig. 22, M) forming R + M. The common vein R + M divides into R_1 and Rs + M. The vein R_1 runs proximal and distad of the stigma on the cephalic margin to slightly beyond the distal end of Rs. The common vein Rs + M divides to produce the cephalic vein Rs, which slopes cephalad to meet the vein R_1; and the caudal vein M, which extends to, but not touching, the distal margin of the wing. A very short crossvein Ir is present between R_1 and Rs. The first abscissa of the vein Rs is atrophied to a faint stub. This produces a large cell IR_1 + IRs. Between Rs and M are two crossveins 2 r-m and 3 r-m. Both of these are atrophied at the centre. Vein M + Cu_1 separates from the

common basal vein, and proceeds to about the centre of the wing, where media (Fig. 22, M) splits from cubitus (Fig. 22, Cu_1). Media runs cephalad to join Rs for a short distance and then separates again to extend to the distal margin. Cubitus proceeds for a short distance and divides into Cu_1a and Cu_1b. The vein Cu_1a extends almost to the distal margin. The vein Cu_1b runs caudad to join the combined anal veins. Between M and Cu_1 are two crossveins, 1 m-cu and 2 m-cu. The cephalic ends of these crossveins and the proximal two-thirds of the media enclosed by the crossveins are atrophied. Between Cu_1 and 1 A is the crossvein cu-a. The extreme caudal portion of this crossvein is atrophied. According to Ross (1936) 2 A + 3 A gradually fused with the anal crossvein (Fig. 22, CV) and then basally along 1 A. The first anal cell thus formed is a reduced loop. The distal margin of the first anal cell is then atrophied, leaving the basal portion of the stub 3 A present. The distal abscissa of 2 A + 3 A joins with 1 A, which runs into Cu_1b. At the junction of Cu_1b and the combined anal veins is a weakened spot. The cubital furrow (Fig. 22, CUF) is evident between the cubital and anal veins. It passes through the atrophied portion of cu-a and the junction of Cu_1b and the combined anal veins. The jugal furrow (Fig. 22, JUF) separates the anal region from the jugal fold. A brown spot is present on the front wing between the greatly atrophied abscissa of Rs and the crossvein 2 r-m. A light infuscated band is evident below the stigma.

The hind wing has a straight cephalic margin, a curving emarginated distal margin, and a rounded caudal margin. A lightly sclerotized crescent-shaped plate (Fig. 25, TG) possessing a few setae is present on the cephalo-proximal area of the wing. This plate appears to correspond to the tegula of the front wing. There are only three axillary sclerites in the base of

the hind wing. The first axillary (Fig. 25, 1 AX), which occupies an oblique position, is irregular in shape and possesses four processes. The proximal margin of the cephaloproximal process articulates with the anterior notal wing process (Fig. 25, ANP_3). The apex of the cephaloproximal process is directed towards a small costal sclerite (Fig. 25, g). This costal sclerite appears to have been detached from the humeral complex (Fig. 25, HC), especially from the base of the costa. The medioproximal process projects dorsally and is associated with the curved scutal fissure (Fig. 25, I_3) at the inner-caudal edge. The caudoproximal process articulates with the edge of the scutum. The distal process is directed ventrally towards the second axillary sclerite (Fig. 25, 2 AX). This latter sclerite is somewhat quadrate in shape and vertical in position. It has a deep cleft on the distal margin, and a slight dorsal ridge on the proximocaudal edge. The cephalic end of the second axillary is directed towards the humeral complex and is associated with the first axillary. The caudal end of this axillary is connected with the third axillary (Fig. 25, 3 AX). The ventral surface of the second axillary rests on the pleural wing process of the metathorax. The somewhat forked and elongate third axillary is oblique in position, with the lateral sides reflected to produce an elongate concavity in the central area. The third axillary has a proximal process, which articulates with the posterior notal wing process (Fig. 25, PNP_3), a cephalic process connected to the second axillary, and a caudal process articulating with the base of the anal veins. In front of the third axillary is a long narrow slightly curved sclerite (Fig. 25, U) on the dorsal surface of the wing base. The humeral complex (Fig. 25, HC) is made up of only the enlarged and united bases of veins C and R + Sc in the hind wing. The base of the costa is hyaline and has a rectangular concavity on the ventral side. Like

the front wing proprioceptive organs (Fig. 25, PCO) are present on the humeral complex. Ventrally the humeral complex has two cephalic processes that articulate with the sides of the basalare of the hind wing. Behind the humeral complex is a sclerotized area with a truncate process directed towards the second axillary. This area appears to be the median plate that has fused with the basal part of the wing proximad of the vein M + Cu_1. The axillary cord at the caudal margin of the hind wing is continuous laterally with the scutellum.

Beneath the base of the hind wing are the basalare (Fig. 20, BA_3) and subalare (Fig. 20, SU_3). The club-like basalare, with an ovoid concavity in the upper margin, is situated cephalad of the pleural wing process. The ventral processes of the humeral complex articulates with the sides of the basalare. The subalare is caudad of the pleural wing process, and is connected with the second axillary sclerite. It is narrow and slightly curved with a ventral process. The ventral border of the subalare, caudad of the ventral process, is produced entad to form a ridge.

Some 22 to 26 humuli (Fig. 27, HU) are present on the costal vein along the cephalic margin of the hind wing. The stigma is greatly reduced. The vein R + Sc (Fig. 27) divides into the veins R_1 and Rs, which join again near the apex of the wing. The bases of C and R + Sc are enlarged to produce the humeral complex. The vein M + Cu_1 divides into M and Cu_1, which extend almost to the distal edge of the wing. Between Rs and M are the crossveins 1 r-m and 3 r-m, which show signs of being atrophied at the caudal end and central area, respectively. A small brown spot is present between these crossveins. One crossvein, m-cu, is between M and Cu_1. This crossvein is atrophied near the centre. The cubital furrow

(Fig. 27, CUF) separates the cubital vein from the anal veins. There are three anal veins in the hind wing. The anal veins 1 A and 2 A meet and extend to near the distal margin. The crossvein cu-a is present between Cu_1 and the combined anal veins. This crossvein is also atrophied at the caudal end. The anal vein 3 A has an enlarged base and extends to the caudodistal area of the wing. The jugal furrow (Fig. 27, JUF) marks off a large anal fold.

2.3 The Abdomen

The setiferous abdomen is broadly joined to the thorax. It carries the external genitalia, and a pair of tapered setiferous appendages, the cerci (Fig. 28, CER) or socii, on the tenth segment. The abdomen consists of ten segments, which are connected by infolded intersegmental membranes.

The spiracles are located on the first eight abdominal segments. Those on the first segment are slightly larger, and located more ventrally than the spiracles on the other segments.

The tergum of the first abdominal segment (Fig. 11, T_1) is narrowly incised on the caudomeson to produce two lateral plates, which are angulated. The sternum of this segment is membranous and invaginated. Abdominal segments 2 to 7 are identical. Each segment has a dorsolateral arch-like tergum (Fig. 23, T) overlapping the sternum (Fig. 23, S). The tergum has a slight median crest, and a transverse line marking off a narrow cephalic part and a wider caudal part. The sternum is plate-like and emarginate mesally on the cephalic margin. The tergum and sternum are separated only by a membranous area.

The eighth tergum (Fig. 23, T 8) is unmodified. The ninth tergum (Fig. 23, T 9), which is narrowed dorsally and overlapped by the eighth tergum, is visible laterally as a large triangular piece. Internally the ninth tergum has a prominent submarginal ridge, the antecosta (Fig. 28, AC). Above the first valvifer (Fig. 28, VLF_1) is a rectangular tergal apodeme (Fig. 28, TAP), projecting entad and ventrad. The tenth tergum (Fig. 23, T 10) or proctiger is a crescent-shaped terminal piece above the anus. The seventh sternum (Fig. 23, S 7) is narrow and forms the subgenital plate. It is produced mesally at the caudal margin to form a bifid plate, the ligamentum (Fig. 23, LG). The eighth and ninth sternites of the female are absent.

2.3.1 The Ovipositor

The origin of the ovipositor of the female has been regarded as modified leg appendages of the eigth and ninth segments. Indications suggest that the external genitalia of insects are sternal in origin (Matsuda, 1958). The first valvifer of the larch sawfly (Figs. 23, 28, VLF_1) is a small triangular plate ventrad of the ninth tergum, and partly concealed by the ventrocaudal part of the eighth tergum. It gives rise cephaladly and ventrally to a narrow first valvula (Fig. 28, VL_1) or lancet containing numerous small pores. A long rod-like groove, the virga (Figs. 28, 29, VI) or ramus, is present on the inner surface near the dorsal margin of the lancet. It curves dorsad to the cephalic angle of the first valvifer. The proximal portion of the lancet has a long radix (Fig. 29, RA), which is mostly membranous with the apical end sclerotized. The radix has on the ventral margin a sclerotized cord the tractium (Fig. 29, TRC), which is enlarged at the heel to form an elongated tangium (Fig. 29, TAG). The tangium is joined by membrane to the ligamentum.

The distal portion of the lancet is the lamnium (Fig. 29, LAM), which tapers gradually to a blunt point. The lamnium is divided into 16 or 17 segments by sutures (Fig. 29, SUT) or annuli. The ventral border of the lamnium is sclerotized to form the sclerora (Fig. 29, SO), which is segregated into abscissae (Fig. 29, ASO) containing one or more pores. The ventral margin of each segment has several small teeth in the sclerora to form the serrula (Fig. 29, SE). The sutures do not generally have a row of spines or ctenidium, but occasionally one or more spines may be present on the central sutures. The uneveness of the proximal sutures would indicate that the spines have been atrophied. The first suture is vertical, the second, third and fourth are angulated, and the remaining sutures are bent or slanted.

The second valvifer (Figs. 23, 28, VLF_2) is a large elongated plate with a medial transverse concavity. It lies ventrad of the first valvifer and beneath the eighth and ninth terga. The second valvifer gives rise cephaladly and ventrally to a narrow pointed second valvula (Fig. 28, VL_2) or lance with a narrow proximal neck, on which is a small dorsal process. This dorsal process will be referred to as the tuberculium (Fig. 28, TU). The lance is divided by ridge-like sutures (Fig. 28, SUT) into 15 segments. Like the lancet it has a large proximal portion, the radix (Fig. 28, RA), and a blade-like distal portion, the lamnium (Fig. 28, LAM). The base of the lance has a group of pores resembling proprioceptive organs. A rod-like groove, the virga (Fig. 28, VI) or ramus, is present near the ventral margin of the lateral surface of the lance. The virga of the lance curves dorsad and is attached to the cephalic angle of the second valvifer. The virga of the lancet is interlocked with the virga of the lance to permit the lancet to slide back and forth. The dorsal edges of the lances are tightly

joined by membrane throughout most of their length. The second valvifer articulates caudally with a broad flat lobe the third valvula (Fig. 28, VL_3), which is separated from the former by a narrow membrane. The two opposing third valvulae from the second valvifers are appressed, and joined tightly at the dorsoproximal margin by membrane to form a sheath. The sheath possesses stiff setae along the ventral and apical margins. The setae on the apical margin of the sheath are longer than those on the ventral margin. A small flange-like projection, the scopa (Fig. 28, SCA), is present on the distal end of the sheath. The second valvifers and the sheath form a protective structure into which the hinged saw retracts in repose.

The first valvifer articulates on its dorsal angle with the ninth tergum and caudoventrally with the second valvifer. The second valvifer has no articulation with the ninth tergum. On the cephalic margin of the first valvifer is a narrow apodeme (Fig. 28, MUP) to which are attached muscles from the eigth tergum. The dorsal edge of the first valvifer projects entad and ventrad to form a flange. The dorsal edge of the second valvifer projects entad to form a ridge, which is more pronounced caudad of the first valvifer. The medial area of the second valvifer has a short internal transverse ridge that bends toward the dorsal margin.

3. THE MALE

Morphologically the male resembles the female except for the genitalia and the terminal segments of the abdomen.

3.1 The Abdomen

The eighth tergum (Fig. 24, T 8) has a fan-shaped convex mesal area at the caudal margin called the procidentia (Fig. 24, PRO). The ninth tergum (Fig. 24. T 9) is reduced and overlapped by the eighth to such an extent as

to expose a small triangular piece on each side in front of the cercus. The tenth tergum (Fig. 24, T 10) resembles that of the female, but it is smaller and less arched. Unlike the female, the eighth and ninth sternites are present in the male. The eighth sternum (Fig. 26, S 8) is emarginated on the cephalic and caudal margins, and is visible only as a triangular caudolateral piece. The ninth sternum (Fig. 26, S 9) is a large plate covering the male genitalia, and forms a concave subgenital plate or hypandrium. It is broadly tapered caudally, and slightly emarginated at the caudal margin. Internally the ninth sternum has a rudimentary antecosta (Fig. 30, AC) and a spur-like median sternal apodeme (Fig. 30, MSA) or spiculum at the cephalic margin, to which are attached muscles for the movement of the genital capsule. The antecosta is evident externally by the antecostal suture.

3.1.1 The Genitalia

The male genitalia is presently believed to be sternal in origin (Matsuda, 1958), and not modified leg appendages of the ninth segment. It is in the form of a heart-shaped capsule of the strophandria type. Genital capsule of this type revolves through a 180° angle soon after the adult emerges. The following description of the male genitalia applies to the condition that occurs after reorientation of the genital capsule. The capsule has at the base, the gonocardo (Figs. 31, 33, GC) a ring-like structure, that narrows cephaladly to a genital foramen (Fig. 33, GF). Ventrally the gonocardo is a mesally emarginated band (Fig. 33, GC) that narrows dorsally (Fig. 31, GC). A small pointed middorsal basal process is present on the gonocardo. A pair of lateral clasper-like appendages are distad of the gonocardo. Each appendage is a gonoforceps consisting of a large curved elongate proximal portion, the gonostipes (Figs. 31, 33, GS), and a roughly

rectangular articulating distal portion, the harpes (Figs. 31, 33, H). The harpes is setiferous and rounded on the lateral surface with the mesal surface flat and slanted. An oval concavity and notch are evident on the ventral surface of the harpes along the proximomesal area and edge respectively. The mesoproximal area of each gonostipes is produced mesad on the ventral aspect to form a triangular structure, the parapenis (Fig. 33, PAP). The two parapenes are fused along a sharply invaginated mesal margin to form the praeputium (Fig. 33, PRP). The line of fusion between the opposing parapenes forms a sharp proximal ental process. The sides of the parapenes distad of the praeputium are invaginated and slope to a distal point. The distal ends of the parapenes are declivous. On the dorsal surface are two structures, which constitute the volsella (Fig. 31, V), and are joined laterally by membrane to the mesal margin of the gonostipes. The large basal portion of each volsella is known as the basivolsella (Fig. 31, BV). The subapical area of the basivolsella possesses a tuft of setae. A slightly curved longitudinal volsellar strut (Fig. 31, VS) is evident in a concavity of the basivolsella. The volsella has two distal lobes, which are not connected by membrane to the gonostipes. The distivolsella (Fig. 31, DV) is the small declivous lateral lobe, which is a continuation of the basivolsella. The larger mesal lobe is the gonolacinia (Fig. 31, GOL), and is connected to the basivolsella by membrane. The small apical portion of the gonolacinia, pointing mesad is the apiceps (Fig. 31, AP). The tail-like basal prolongation of the gonolacinia is the basiura (Fig. 31, BR). The central structure between the volsellae is the aedeagus consisting of a median membranous area, and a pair of elongated lateral penis valves (Figs. 31, 33, PV). The penis valves are hinged by membrane along the ventrodistal surface. Each penis valve has a sclerotized tail-like proximal part, the

valvura (Fig. 32, VR), and a body-like distal part at the valviceps (Fig. 32, VC). The valvura is attached to the genital capsule by membrane and muscle. It has an impressed groove, which is bulbous at the base, and narrows to a line in the direction of the lateroproximal corner of the valviceps. This groove will be called the valvural stria (Fig. 32, VST). The valviceps has a longitudinal sclerotized mesal thickening, the valvar strut (Fig. 32, VV), in addition to a mesal flap, the pseudoceps (Fig. 32, PSC), and a lateral flap, the paravalva (Fig. 32, PR). The paravalva terminates into a slight spur, the valvispina (Fig. 32, VA). The pseudoceps has the distal edge thickened to form a slight narrow hood over the valvispina. This structure will be called the pseudocepal thickening (Fig. 32, PST). A ridge (Fig. 32, PS) is present extending slightly diagonally from the valvispina to the valvar strut. This structure will be called the paravalvar strut. Between the valviceps and the valvura is a rudimentary lateral projection, the ergot (Fig. 32, EG).

ACKNOWLEDGMENTS

I would like to express my appreciation to W. A. Reeks and R. M. Prentice for the reading of this manuscript. I am indebted to J. A. Drouin for his assistance in the final preparation of the illustrations.

REFERENCES

Arora, G. L. 1953. The external morphology of Diprion pini (L.) (Symphata-Hymenoptera).
East Panjab Uni. Res. Bull. 25:1-21.

Arora, G. L. 1956. The Relationship of the Symphyta (Hymenoptera) to other orders of insects on the basis of adult external morphology.
East Panjab Uni. Res. Bull. 90:85-119.

Bigelow, R. S. 1954. Morphology of the face in the Hymenoptera.
Can. J. Zool. 32:378-392.

Bird, R. D. 1926. The external anatomy of the adult of Hoplocampa halcyon Nort. (Hym. Tenthred.).
Ann. Ent. Soc. Amer. 19:268-277.

Coppel, H. C. and Leius, K. 1955. History of the larch sawfly, with notes on origin and biology.
Can. Ent. 87:103-109.

DuPorte, E. M. 1946. Observations on the morphology of the face in insects.
J. Morphol. 79:371-418.

DuPorte, E. M. 1957. The comparative morphology of the insect head.
Ann. Rev. Ent. 2:55-70.

Hewitt, C. G. 1912. The large larch sawfly (Nematus erichsonii) with an account of its parasites, other natural enemies and means of control.
Canada, Dept. Agr., Ento. Bull. 5:42 pp.

Marlatt, C. L. 1896. Revision of the Nematinae of North America.
Bull. U.S. Dept. Agr. Div. Ent. Tech. Ser. 3:135 pp.

Matsuda, R. 1958. On the origin of the external genitalia of insects.
Ann. Ent. Soc. Amer. 51:84-94.

Michener, C. D. 1944. Comparative external morphology, phylogeny, and a classification of the bees (Hymenoptera).
Bull. Amer. Mus. Nat. Hist. 82:157-326.

Packard, A. S. 1890. Fifth Report U.S. Ent. Comm., revised and enlarged edition of Bull. No. 7, on insects injurious to forest and shade trees. 886-887.

Reeks, W. A. 1937. The morphology of the adult of Diprion polytomum (Hartig).
Can. Ent. 69:257-264.

Richards, O. W. 1956. An interpretation of the ventral region of the Hymenopterous thorax.
Proc. Roy. Ent. Soc. Lond. 31:99-104.

Rivard, I. 1955. Contribution to the morphology of a pine web-spinning sawfly, Cephalacia marginata Middlekauff (Hymenoptera: Pamphiliidae).
Can. Ent. 87:382-399.

Ross, H. H. 1936. The ancestry and wing venation of the Hymenoptera.
Ann. Ent. Soc. Amer. 29:99-111.

Ross, H. H. 1937. A generic classification of the Nearctic sawflies (Hymenoptera, Symphata).
Illinois Biol. Monogr. 5:173 pp.

Ross, H. H. 1945. Sawfly genitalia: Terminology and study techniques.
Ent. News 56:261-268.

Smulyan, M. T. 1923. New England sawflies of the genus Tenthredella Rohwer.
Proc. Boston Soc. Nat. Hist. 36:383-465.

Snodgrass, R. E. 1933. Morphology of the insect abdomen. Part II. The genital ducts and the ovipositor.
Smith. Misc. Coll. 89:148 pp.

Snodgrass, R. E. 1935. Principles of Insect Morphology.
McGraw-Hill Book Co. Inc., N. Y. 667 pp.

Snodgrass, R. E. 1956. Anatomy of the Honey Bee.
Comstock Pub. Ass. Ithaca, N. Y. 334 pp.

PLATE I

ADULT OF LARCH SAWFLY
Pristiphora erichsonii (Htg.)

Fig. 1.--Cephalic aspect of head

Fig. 2.--Caudal aspect of head

Fig. 3.--Cephalic aspect of right maxilla

Fig. 4.--Cephalic aspect of labium

Fig. 5.--Cephalic aspect of left and right mandibles

Fig. 6.--Entolateral aspect of head

Fig. 7.--Entodorsal aspect of prothorax

Fig. 8.--Caudal aspect of labrum

Fig. 9.--Lateral aspect of antenna

ABBREVIATIONS

AGL	alaglossa
AMA	anterior mandibular articulation
AN	antennifer
ANT	antenna
ANTS	antennal socket
AS	antennal suture
AT	anterior tentorial arm
ATP	anterior tentorial pit
BL	bulbus
BS	basisternum
c	apodemal ridge of proepisternum
CD	cardo
CE	compound eye
CGB	clypeogenal bridge
CGI	clypeogenal inflection
CL	clypeus
CLS	clypeolabral suture
CS	coronal suture
d	cervical apodeme of proepisternum
DT	dorsal tentorial arm
e	odonoideal articulation
EDS	endosternum
EPM	epimeron
EPS	episternum
F	frons
FCS	frontoclypeal sulcus
FGI	frontogenal inflection
FGS	frontogenal sulcus
FL	flagellum
FP	frontoparietal region
FS	frontal suture
GE	gena
GL	galea
HP	hypopharynx
HPA	horizontal plate of sternal apophysis
HS	hypostomal suture
HST	hypostoma
LA	labrum
LC	lacinia
LO	lateral ocellus
LP	labial palpus
LS	lateral sulcus
LU	labium
MA	mandible
MO	median ocellus
MUP	muscle apodeme
MX	maxillaria
MXP	maxillary palpus
OC	occiput
OCF	occipital foramen
OD	odontoidea
OS	ocular suture
PAC	paracoila
PD	pedicel
PFR	palpifer
PG	postgena
PGL	paraglossa
PGR	palpiger
PHS	pharyngeal sclerite
PLA	pleural arm
PLS	pleural sulcus
PM	postmentum
PMA	posterior mandibular articulation
PMS	postmental sclerite
PO	postocciput
POA	postocellar area
POS	postoccipital sulcus
PRM	prementum
PTP	posterior tentorial pit
SC	scape
ST	stipes
TB	tentorial bridge
TM	tentorial macula
TOR	torma
TS	transverse suture
TT	tentorial thickening
VE	vertex
VPA	vertical plate of sternal apophysis

PLATE I

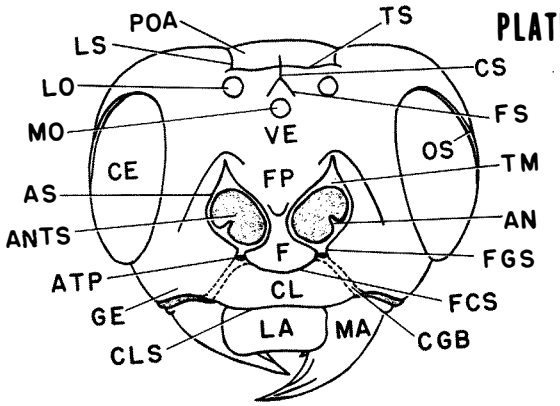

1

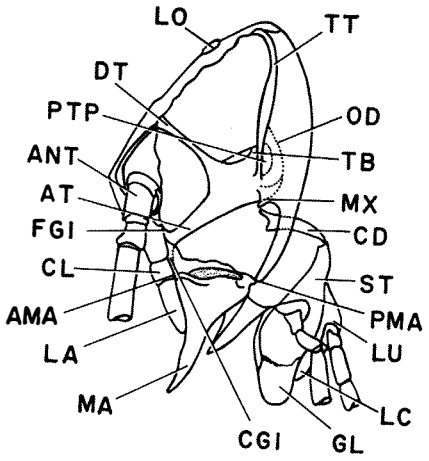

6

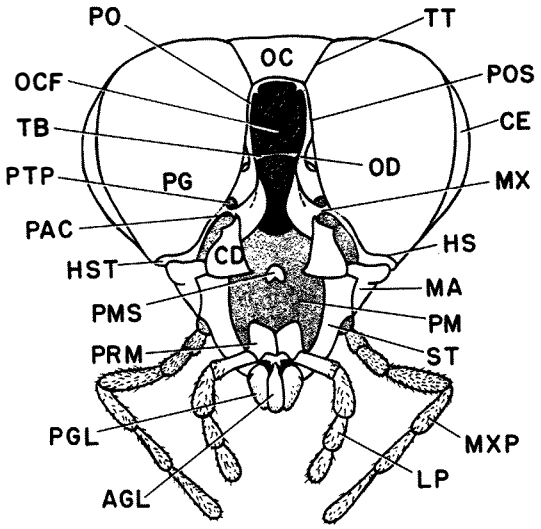

2

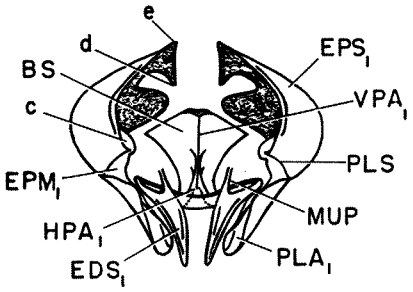

7

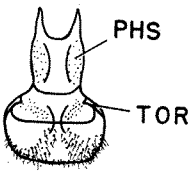

8

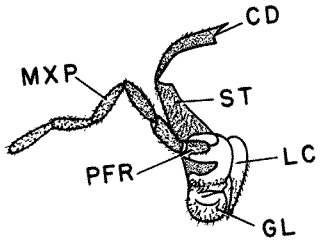

3

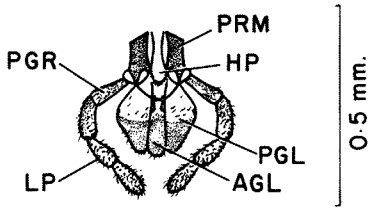

4

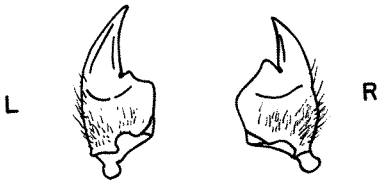

5

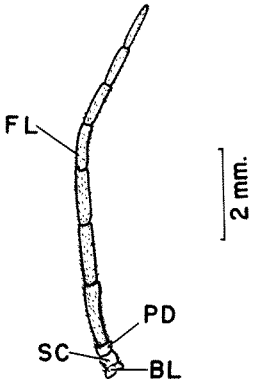

9

1 mm.

PLATE II

ADULT OF LARCH SAWFLY
Pristiphora erichsonii (Htg.)

Fig. 10.--Ventral aspect of thorax

Fig. 11.--Dorsal aspect of thorax

Fig. 12.--Caudal aspect of left metathoracic leg

Fig. 13.--Dorsal aspect of pretarsus

Fig. 14.--Ventral aspect of pretarsus

ABBREVIATIONS

AES	anepisternum	ORB	orbicula
AOS	anterior oblique sulcus	PAR	parapsis
AR	arolium	PC	pleural cleft
ASP	anterolateral mesoscutal process	PES	presternum
AU	auxilia	PF	parapsidal furrow
BS	basisternum	PH	phragma
BSC	basicoxite	PL	planta
CA	camera	PRN	pronotum
CBS	central portion of basisternum	PRS	prescutum
CN	cenchrus	PRT	pretarsus
CW	claw	PTG	posttergite
CX	coxa	PTN	postnotum
d	cervical apodeme of proepisternum	SCL	scutellum
DCM	discrimen	SCUT	scutum
DP	discrimenal pit	SP	thoracic spiracle
e	odontoideal articulation	SPL	sclerotized plate
EDS	endosternum	SS	spinisternum
ENS	external notal sulcus	SUL	sulcus
EPC	epicnemium	T	abdominal tergite
EPM	epimeron	TAR	tarsus
EPS	episternum	TG	tegula
FM	femur	TI	tibia
FRS	furcasternum	TIS	tibial spur
G	internal disk of mesepisternum	TP	tarsal pulvillus
I	scutal fissure	TR	trochanter
L	lip of phragmatal inflection	TRO	trochantin
MS	median sulcus	UF	unguifer
NO	notaulix	UTP	unguitractor plate

PLATE II

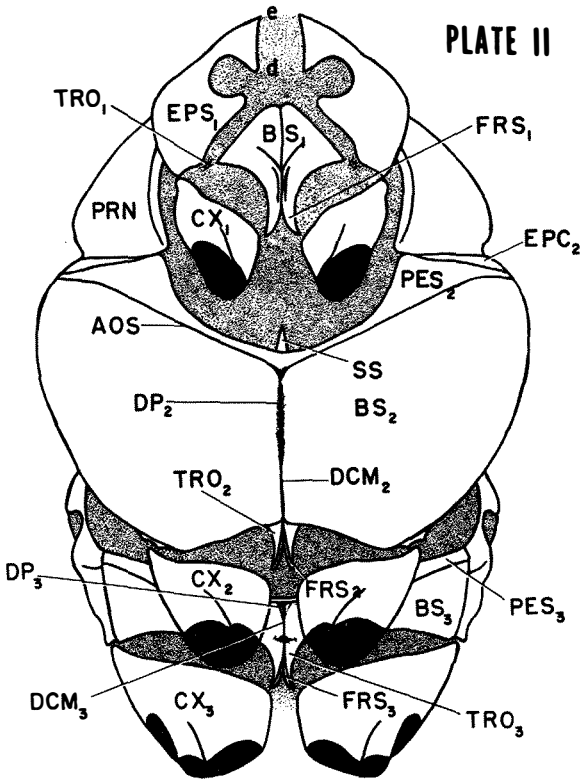

10

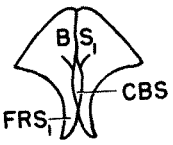

10a

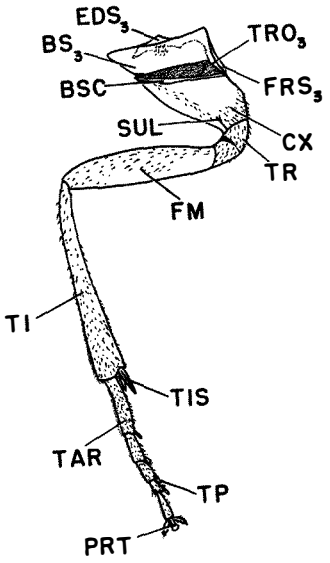

12

2 mm.

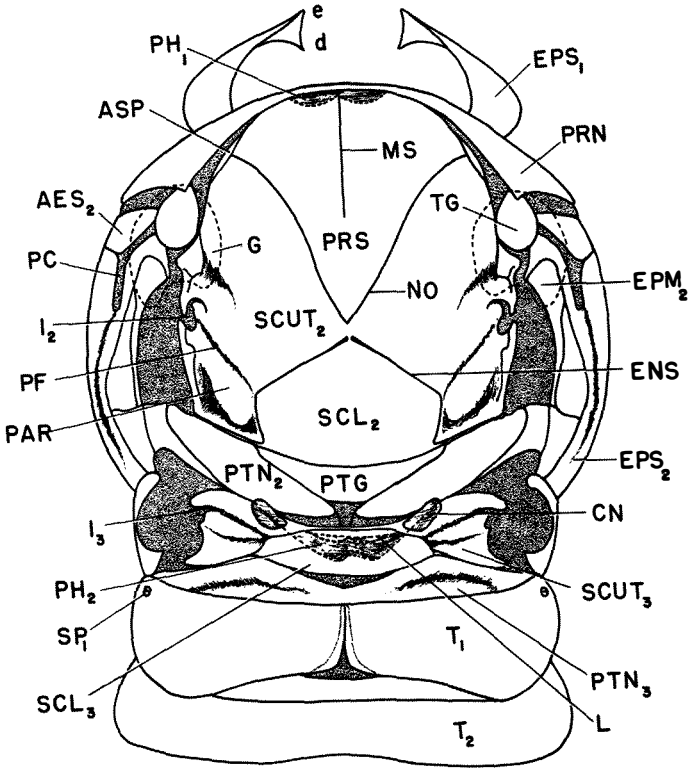

11

1mm.

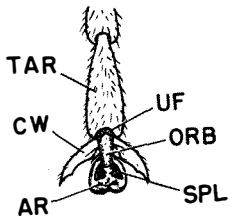

13

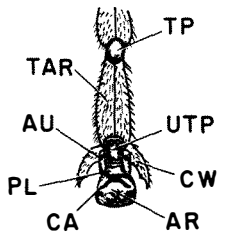

14

0·5 mm.

PLATE III

ADULT OF LARCH SAWFLY
Pristiphora erichsonii (Htg.)

Fig. 15.--Lateral aspect of thorax

Fig. 16.--Entoventral aspect of mesonotum

Fig. 17.--Entoventral aspect of metanotum

Fig. 18.--Entolateral aspect of meso- and metathorax

ABBREVIATIONS

AEM	anepimeron
AES	anepisternum
AKA	anterior pleural apodeme
AOR	anterior oblique ridge
AOS	anterior oblique sulcus
APA	anterior presternal apodeme
ASI	anterolateral mesoscutal inflection
BS	basisternum
CN	cenchrus
CR	convergent ridge
CSC	cervical sclerite
CX	coxa
DMI	dorsal mesepimeral inflection
EDS	endosternum
EPC	epicnemium
EPM	epimeron
EPR	epicnemial ridge
EPS	episternum
ER	epimeral ridge
ES	epimeral sulcus
ESU	epicnemial sulcus
FRS	furcasternum
G	internal disk of mesepisternum
HPA	horizontal plate of sternal apophysis
I	scutal fissure
INR	internal notal ridge
KEM	katepimeron
KES	katepisternum
LSI	lateroposterior mesoscutal inflection
MR	median ridge
PA	pleural articulation
PAR	parapsis
PC	pleural cleft
PES	presternum
PH	phragma
PLA	pleural arm
PLR	pleural ridge
PLS	pleural sulcus
PN	pronotal lobe
PRN	pronotum
PRS	prescutum
PTG	posttergite
PTN	postnotum
R	mesepimeral ridge
RD	posterior marginal fold of scutellum
SA	sternal articulation
SAP	subalar pit
SCL	scutellum
SCUT	scutum
SP	thoracic spiracle
SPN	spina
T	abdominal tergite
TA	trochantinal articulation
TAP	tergal apodeme
TRO	trochantin
VPA	vertical plate of sternal apophysis
WP	pleural wing process

PLATE III

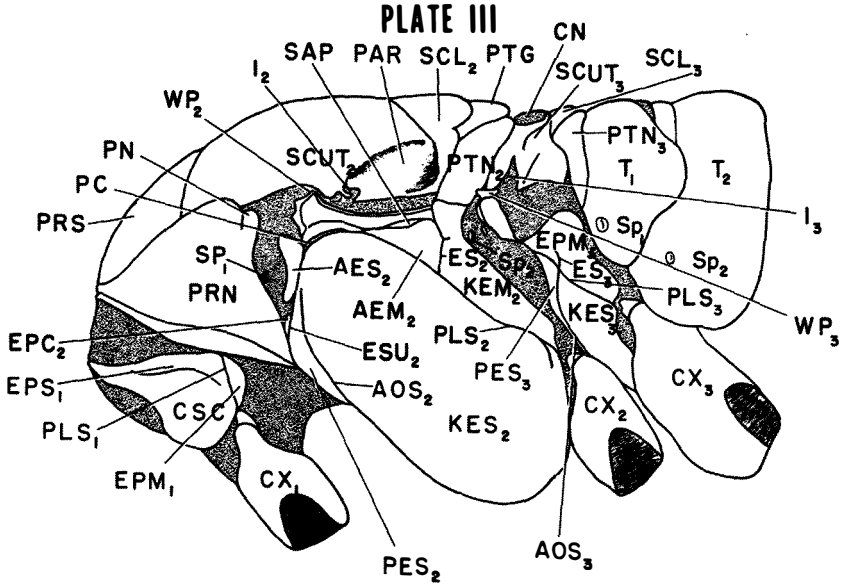

15

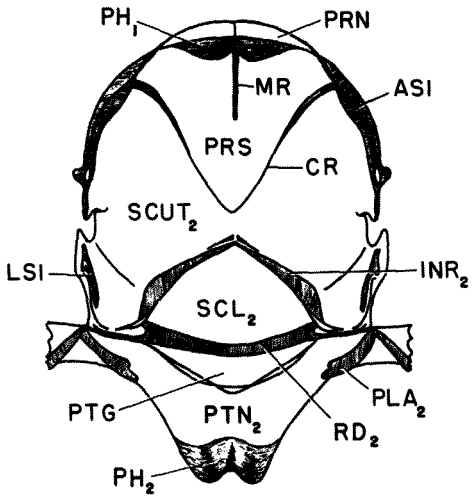

16

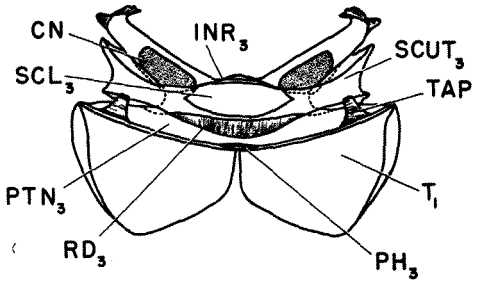

17

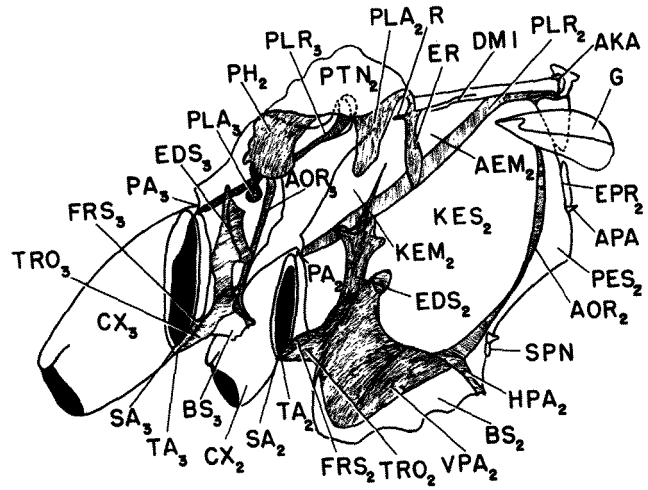

18

1 mm.

PLATE IV

ADULT OF LARCH SAWFLY
Pristiphora erichsonii (Htg.)

Fig. 19.--Entodorsal aspect of meso- and metathorax

Fig. 20.--Lateral aspect of the epipleurites of the meso- and metathorax

Fig. 21.--Dorsal aspect of the base of front wing

Fig. 22.--Dorsal aspect of front wing

ABBREVIATIONS

a	distal costal sclerite of mesothoracic wing
A	anal vein
AEM	anepimeron
AES	anepisternum
ANP	anterior notal wing process
AOR	anterior oblique ridge
AOS	anterior oblique sulcus
ASP	anterolateral mesoscutal process
AX	axillary sclerite
AXC	axillary cord
b	proximal costal sclerite of mesothoracic wing
BA	basalare
C	costa
CF	coupling fold
cu-a	cubitoanal crossvein
CUF	cubital furrow
CV	crossvein
CX	coxa
EDS	endosternum
EPC	epicnemium
EPM	epimeron
ESU	epicnemial sulcus
f	sclerotized plate of mesothoracic wing
G	internal disk of mesepisternum
HC	humeral complex
HPA	horizontal plate of sternal apophysis
I	scutal fissure
JUF	jugal furrow
KEM	katepimeron
KES	katepisternum
M	media
m-cu	mediocubital crossvein
MP	median plate
NO	notaulix
PC	pleural cleft
PCO	proprioceptive organs
PES	presternum
PLA	pleural arm
PLR	pleural ridge
PLS	pleural sulcus
PNP	posterior notal wing process
PRS	prescutum
PTG	posttergite
r	radial crossvein
R	radius
r-m	radiomedial crossvein
Rs	radial sector
Sc	subcosta
SCL	scutellum
SCUT	scutum
SP	thoracic spiracle
SPN	spina
STG	stigma
SU	subalare
TG	tegula
VPA	vertical plate of sternal apophysis

PLATE IV

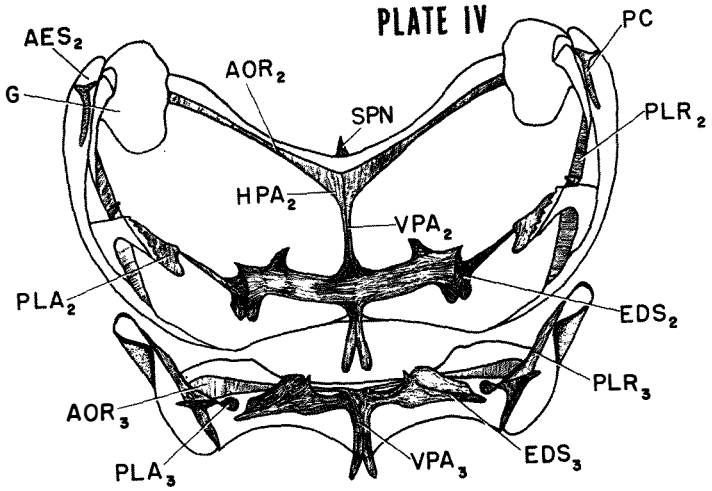

19

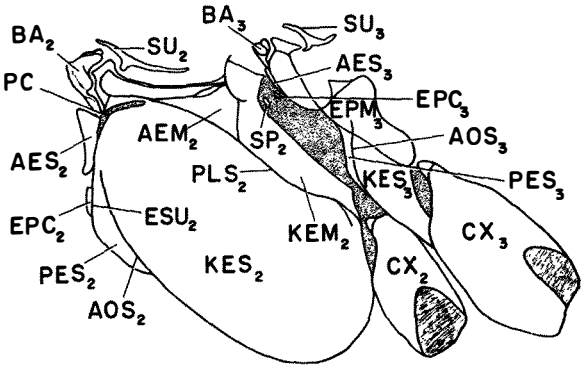

20

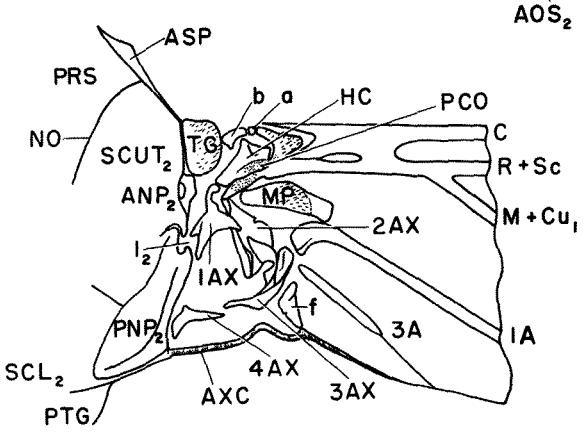

21

1 mm.

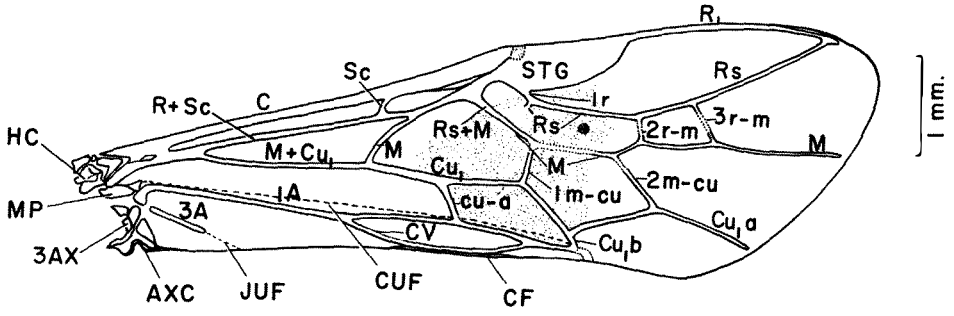

1 mm.

22

PLATE V

ADULT OF LARCH SAWFLY
Pristiphora erichsonii (Htg.)

Fig. 23.--Lateral aspect of female abdomen

Fig. 24.--Dorsal aspect of terminal segments of male abdomen

Fig. 25.--Dorsal aspect of the base of hind wing

Fig. 26.--Lateral aspect of terminal segments of male abdomen

Fig. 27.--Dorsal aspect of hind wing

ABBREVIATIONS

A	anal vein
ANP	anterior notal wing process
AX	axillary sclerite
C	costa
CER	cercus
CN	cenchrus
Cu	cubitus
cu-a	cubitoanal crossvein
CUF	cubital furrow
g	costal sclerite of metathoracic wing
H	harpes
HC	humeral complex
HU	hamuli
I	scutal fissure
JUF	jugal furrow
LG	ligamentum
M	media
m-cu	mediocubital crossvein
MP	median plate
PCO	proprioceptive organs
PNP	posterior notal wing process
PRO	procidentia
PTN	postnotum
PV	penis valve
R	radius
r-m	radiomedial crossvein
Rs	radial sector
S	abdominal sternite
Sc	subcosta
SCL	scutellum
SCUT	scutum
Sp	abdominal spiracle
T	abdominal tergite
TG	tegula
U	sclerite of metathoracic wing
VL	valvula
VLF	valvifer

PLATE V

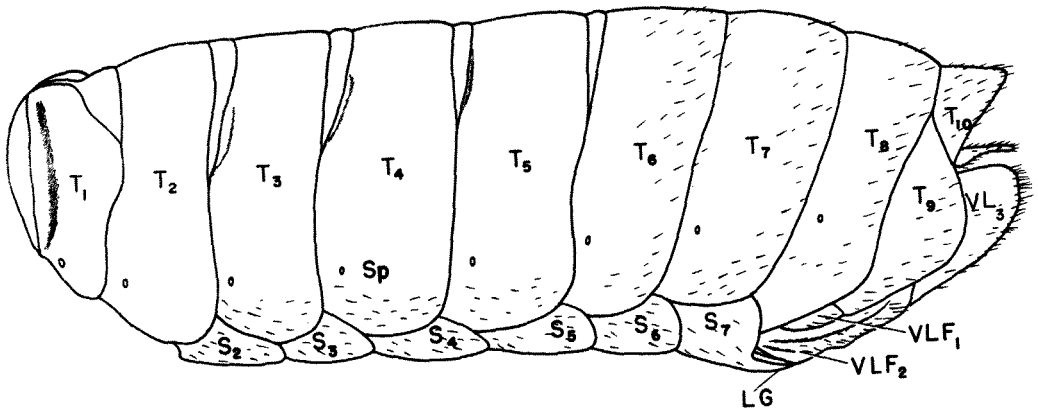

23

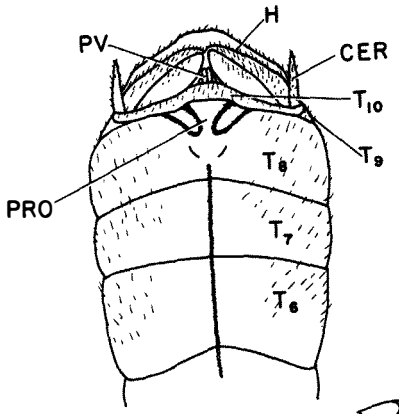

24

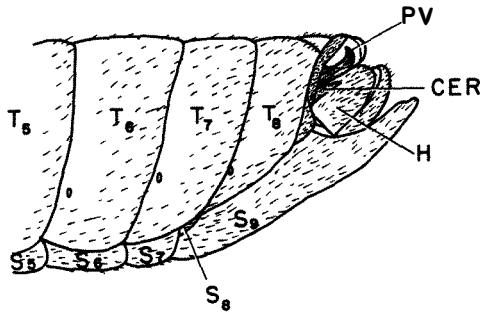

26

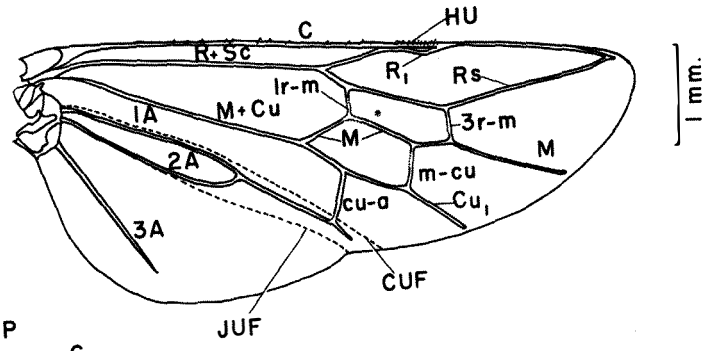

27

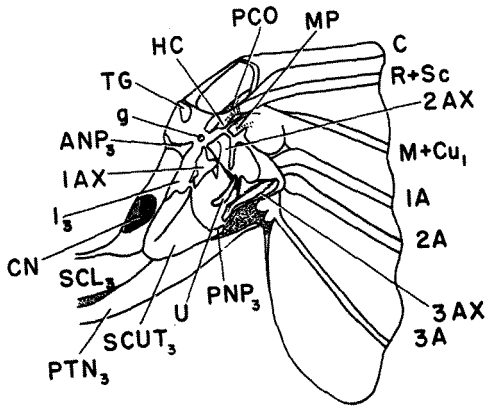

25

PLATE VI

ADULT OF LARCH SAWFLY
Pristiphora erichsonii (Htg.)

Fig. 28.--Entolateral aspect of female ovipositor

Fig. 29.--Lateral aspect of lancet

Fig. 30.--Entodorsal aspect of terminal segment of male abdomen

Fig. 31.--Dorsal aspect of male genitalia

Fig. 32.--Lateral aspect of penis valve

Fig. 33.--Ventral aspect of male genitalia

ABBREVIATIONS

AC	antecosta
AP	apiceps
ASO	abscissa of sclerora
BR	basiura
BV	basivolsella
CER	cercus
DV	distivolsella
EG	ergot
GC	gonocardo
GF	genital foramen
GOL	gonolacinia
GS	gonostipes
H	harpes
LAM	lamnium
MSA	median sternal apodeme
MUP	muscle apodeme
PAP	parapenis
PR	paravalva
PRP	praeputium
PS	paravalvar strut
PSC	pseudoceps
PST	pseudocepal thickening
PV	penis valve
RA	radix
S	abdominal sternite
SCA	scopa
SE	serrula
SO	sclerora
SUT	suture
T	abdominal tergite
TAG	tangium
TAP	tergal apodeme
TRC	tractium
TU	tuberculium
V	volsella
VA	valvispina
VC	valviceps
VI	virgae
VL	valvula
VLF	valvifer
VR	valvura
VS	volsellar strut
VST	valvural stria
VV	valvar strut

PLATE VI

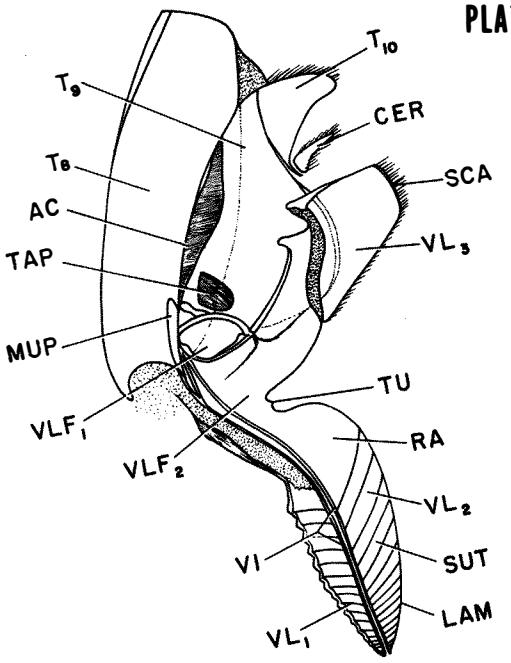

28

1mm.

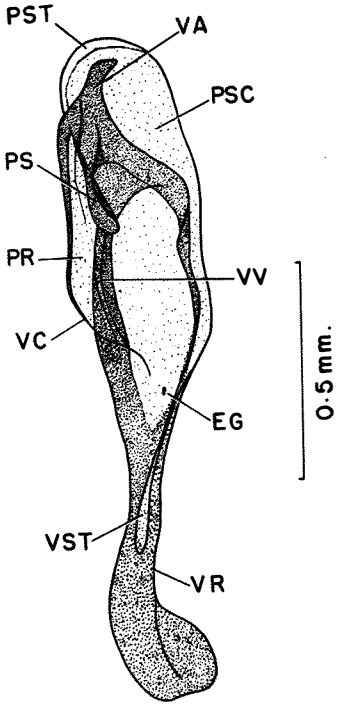

32

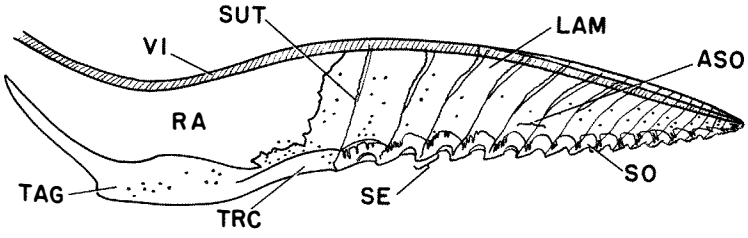

29

0·5 mm.

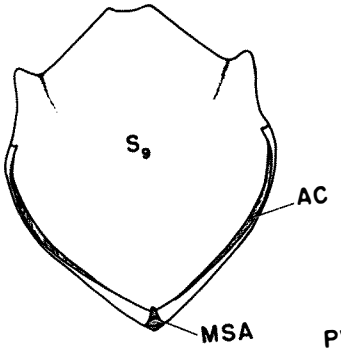

30

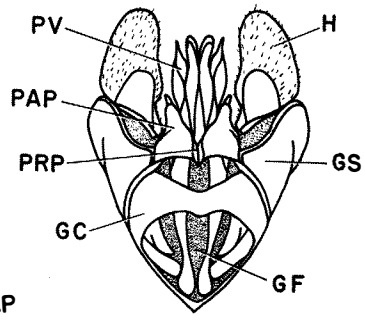

33

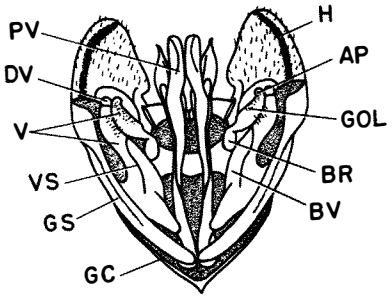

31

1mm.